Arch. Metall. Mater. **63** (2018), 4, 1629-1636

DOI: 10.24425/amm.2018.125086

A. IRFAN*#, A.R. CHAUDHRY**, A.G. AL-SEHEMI*, S. MUHAMMAD***,
R. JIN****, S. TANG*****

TUNING THE CHARGE TRANSFER AND OPTOELECTRONIC PROPERTIES OF 4,6-DI(THIOPHENE-2-YL)PYRIMIDINE VIA OLIGOCENOTHIOPHENE SUBSTITUTION

Five new derivatives of 4,6-di(thiophen-2-yl)pyrimidine (DTP) were designed by structural modification with the aim to tune the electro-optical and charge transfer properties. The effect of oligocene and oligocenothiophene incorporation/substitution was investigated on various properties of interests. The smaller hole reorganization energy revealed that compounds **1**-**5** might be good hole transfer contenders. The smaller hole reorganization energy of newly designed five DTP derivatives than the pentacene showed that prior compounds might be good/comparable hole transfer materials than/to that of pentacene. The computed electron reorganization energy of DTP derivatives **1**-**5** are 124, 185, 93, 95 and 189 meV smaller than the meridional-tris (8-hydroxyquinoline) aluminum (*mer*-Alq3) illuminating that electron mobility of these derivatives might be better/comparable than/to referenced compound.

Keywords: Organic semiconductors, Oligocene, Density functional theory, Optoelectronic properties, Charge transfer properties

1. Introduction

Since the last three decades a lot of development has been made in organic semiconductor devices. The organic π-conjugated materials have been extensively studied due to their potential applications in electronics and optoelectronics [1-4], e.g., organic field-effect transistors (OFETs), organic thin-film transistors (OTFTs), organic light-emitting diodes (OLEDs), photovoltaic and sensors [5-7]. In organic π-conjugated materials the electron-phonon interactions are equivalent to the electronic interactions which can be addressed by reorganization energy (λ) that is inversely proportional to the charge transfer rate [8]. The charge transfer rate can be increased by enhancing the intra-molecular charge transfer (ICT), minimizing the polarization and structural variation by incorporating the electron-deficient moieties [9,10]. Small organic molecules are mainly cost-effective, environmental friendly and ease to fabricate [11]. Moreover, excellent electro-optical and charge transfer properties can be achieved by chain alignment of small organic molecules. The favorable chain conformation [12,13], molecular structure with suitable highest occupied molecular orbital (HOMO), lowest unoccupied molecular orbital (LUMO), electron affinity (EA) and ionization potential (IP) of organic molecules are particularly profitable for improved electronic applications [14]. Polyacenes are utmost favorable molecules to fabricate proficient OFETs [15,16]. Furthermore, the end groups, π-conjugated cores and heteroatoms substitution are favorable strategies to modify the small organic molecules and to control the electrical properties [17].

In our previous study, it has been shown that 4,6-di(thiophen-2-yl)pyrimidine (DTP) is a good building block to design efficient optoelectronic materials [18]. With the aim to tune the electro-optical and charge transfer properties, thiophene and oligocene moieties have been incorporated on DTP by chain alignment technique. Here, five new star shaped systems have been designed by structural modification the longitudinal wings, i.e.,

(2,5-di(thiophen-2-yl)-4,6-di (tetracenothiophen-2-yl)pyrimidine) (**1**),
(2,5-di(benzothiophen-2-yl)-4,6-di (tetracenothiophen-2-yl)pyrimidine) (**2**),
2,5-di(naphthothiophen-2-yl)-4,6-di (tetracenothiophen-2-yl)pyrimidine (**3**),
2,5-di(anthracenothiophen-2-yl)-4,6-di (tetracenothiophen-2-yl)pyrimidine (**4**)
and
2,4,5,6-tetrakis(tetracenothiophen-2-yl)pyrimidine (**5**),

see Fig. 1. The electronic properties (frontier molecular orbitals (FMOs), total/partial density of states (T/PDOS) and molecular electrostatic potentials (MEP)), optical properties (absorption spectra (λ_{abs}), fluorescence spectra (λ_f), major contributions/

* KING KHALID UNIVERSITY, FACULTY OF SCIENCE, DEPARTMENT OF CHEMISTRY, ABHA 61413, P.O. BOX 9004, SAUDI ARABIA
** DEANSHIP OF SCIENTIFIC RESEARCH, UNIVERSITY OF BISHA, BISHA 61922, P.O. BOX 551, SAUDI ARABIA
*** KING KHALID UNIVERSITY, FACULTY OF SCIENCE, DEPARTMENT OF PHYSICS, ABHA 61413, P.O. BOX 9004, SAUDI ARABIA
**** CHIFENG UNIVERSITY, COLLEGE OF CHEMISTRY AND CHEMICAL ENGINEERING, CHIFENG 024000, CHINA
***** JILIN AGRICULTURE UNIVERSITY, COLLEGE OF LIFE SCIENCE, CHINA
# Corresponding author: irfaahmad@gmail.com

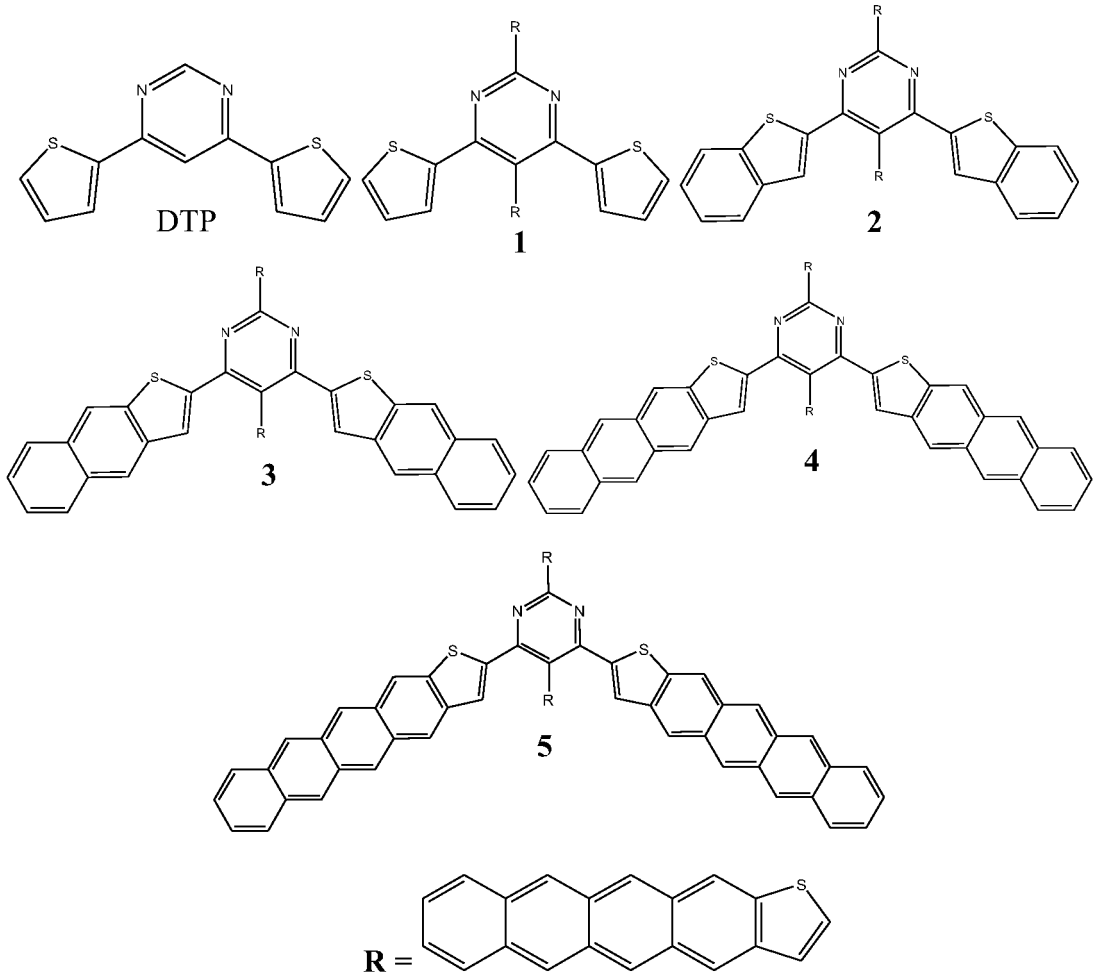

Fig. 1. The structures of DTP and its derivatives investigated in the presented study

transitions of excitations and charge transfer properties (vertical/adiabatic EA (EAv/a, vertical/adiabatic IP (IPv/a), and hole/electron reorganization energies ($\lambda(h)/\lambda(e)$) were studied thoroughly.

2. Methodology

It is well-known that B3LYP is a sound functional of density functional theory (DFT) [19-22] which reproduce the experimental structural data than the other functionals [23]. Moreover, Petersson et al. showed that B3LYP functional [24] and 6-31G** basis set [25] is reasonable for the reproduction of structural parameters. Thus to keep in mind the reliability of B3LYP/6-31G** level, here the ground state (S_0) geometries of the neutral, anion and cation were optimized at the same level. The real frequency values of DTP and its derivatives **1-5** showed that optimized structures are the stable ones with the lowest energy which are reliable for further calculations. The excited state (S_1) geometries were optimized at time dependent DFT (TDDFT) [26] at TD-B3LYP/6-31G** level of theory. Likewise, the TDDFT was confirmed an effective approach to reproduce the experimental absorption (λ_a) and fluorescence spectra (λ_f) successfully [27, 28]. The λ_a and λ_f were computed by applying the TD-B3LYP/6-31G** level of theory [29]. According to the Marcus theory charge transfer rate can be defined as [30].

$$W = t^2/h(\pi/\lambda k_B T)^{1/2} \exp(-\lambda/4k_B T) \quad (1)$$

The transfer integral (t) and reorganization energy (λ) are noteworthy parameters which help to understand the charge transfer behavior. Usually, t needs to be maximized whereas λ to be small for significant transfer. The $\lambda_{rel}^{(1)}$ and $\lambda_{rel}^{(2)}$ are the main parts of λ which are geometry relaxation energy from neutral to charged state and charged to neutral state, respectively [31].

$$\lambda = \lambda_{rel}^{(1)} + \lambda_{rel}^{(2)} \quad (2)$$

The λ can be evaluated as [32].

$$\lambda = \lambda_{rel}^{(1)} + \lambda_{rel}^{(2)} = [E^{(1)}(L^{+/-}) - E^{(0)}(L^{+/-})] + [E^{(1)}(L) - E^{(0)}(L)] \quad (3)$$

where, $E^{(0)}(L)$ is the S_0 energy of the neutral state, $E^{(0)}(L^{+/-})$ is energy of charged states, $E^{(1)}(L^{+/-})$ is the energy of the charged state at the geometry of the optimized neutral molecule and $E^{(1)}(L)$ is the energy of the neutral molecule at the optimized charged geometry. The B3LYP/6-31G** level of theory was used to calculate the IPa/v and EAa/v [33, 34]. All the calculations were performed by Gaussian 09 package [35].

3. Results and discussion

3.1. Electronic properties

In Table 1, the energies of the FMO, i.e., HOMO/LUMO energies (E_{HOMO}/E_{LUMO}) and HOMO-LUMO energy gaps (E_g) have been tabulated. The calculated E_{HOMO}/E_{LUMO} of DTP were –6.19/–1.94 at S_0 and –6.02/–2.10 eV at S_1, respectively [18]. The computed E_{HOMO}/E_{LUMO} at the S_0 of **1**-**5** are –4.65/–2.42, –4.67/–2.46, –4.68/–2.48, –4.68/–2.49, and –4.68/–2.60 while at S_1 –4.46/–2.68, –4.45/–2.64, –4.46/–2.65, –4.46/–2.66, and –4.46/–2.68, respectively. It can be found that elongation of oligocene core has moderate effect on the E_{LUMO} of the S_0 which decreases by increasing the oligocene moieties. The tendency in the E_g at the S_0 has been observed as DTP (4.25) > **1** (2.29) > **2** (2.27) > **3** (2.25) > **4** (2.23) > **5** (2.16) eV. The E_g is slightly decreased after substituting the benzene, naphthalene, anthracene and tetracene.

The electron injection energy (EIE) can be calculated as LUMO energy − work of function Aluminum (i.e., 4.08 eV) [36]. The EIE in DTP is 2.14 eV = −1.94 − (−4.08). The calculated EIE in **1**-**5** is 1.66, 1.62, 1.60, 1.59 and 1.48 eV, respectively. The hole injection energy (HIE) for DTP can be calculated as 2.11 eV (= −4.08 − (−6.19)). The calculated HIE in **1**-**5** is 0.57, 0.59, 0.60, 0.60 and 0.60 eV, respectively. From these results, it can be found that by lowering the LUMO energy level the electron injection ability can be enhanced. Similarly, by increasing the HOMO energy level hole injection ability can be improved. Generally, by incorporating the oligocene moieties (elongation of π-bridge) the hole and electron injection barrier of **1**-**5** reduced as compared to the parent compound revealing that prior compounds would be proficient hole and electron transfer materials than the later one.

TABLE 1

The HOMO energies (E_{HOMO}), LUMO energies (E_{LUMO}), and energy gaps (E_{gap}) of DTP and its derivatives (in eV) at the ground and first excited states at the B3LYP/6-31G** and TD-B3LYP/6-31G** levels of theory, respectively

Complexes	Ground state				First excited state		
	E_{HOMO}	E_{LUMO}	[a]E_{LUMO+n}	E_g	E_{HOMO}	E_{LUMO}	E_g
DTP	–6.19	–1.94	—	4.25	–6.02	–2.10	3.92
1	–4.65	–2.42	–2.36	2.29	–4.46	–2.68	1.78
2	–4.67	–2.46	–2.40	2.27	–4.45	–2.64	1.81
3	–4.68	–2.48	–2.43	2.25	–4.46	–2.65	1.81
4	–4.68	–2.49	–2.45	2.23[b]	–4.46	–2.66	1.79
5	–4.68	–2.60	–2.52	2.16	–4.46	–2.68	1.78

[a]E_{LUMO+n} is E_{LUMO+1} except for **4** where it means E_{LUMO+2} (contributing in the major transition); [b]E_{gap} between E_{HOMO} and E_{LUMO+2}

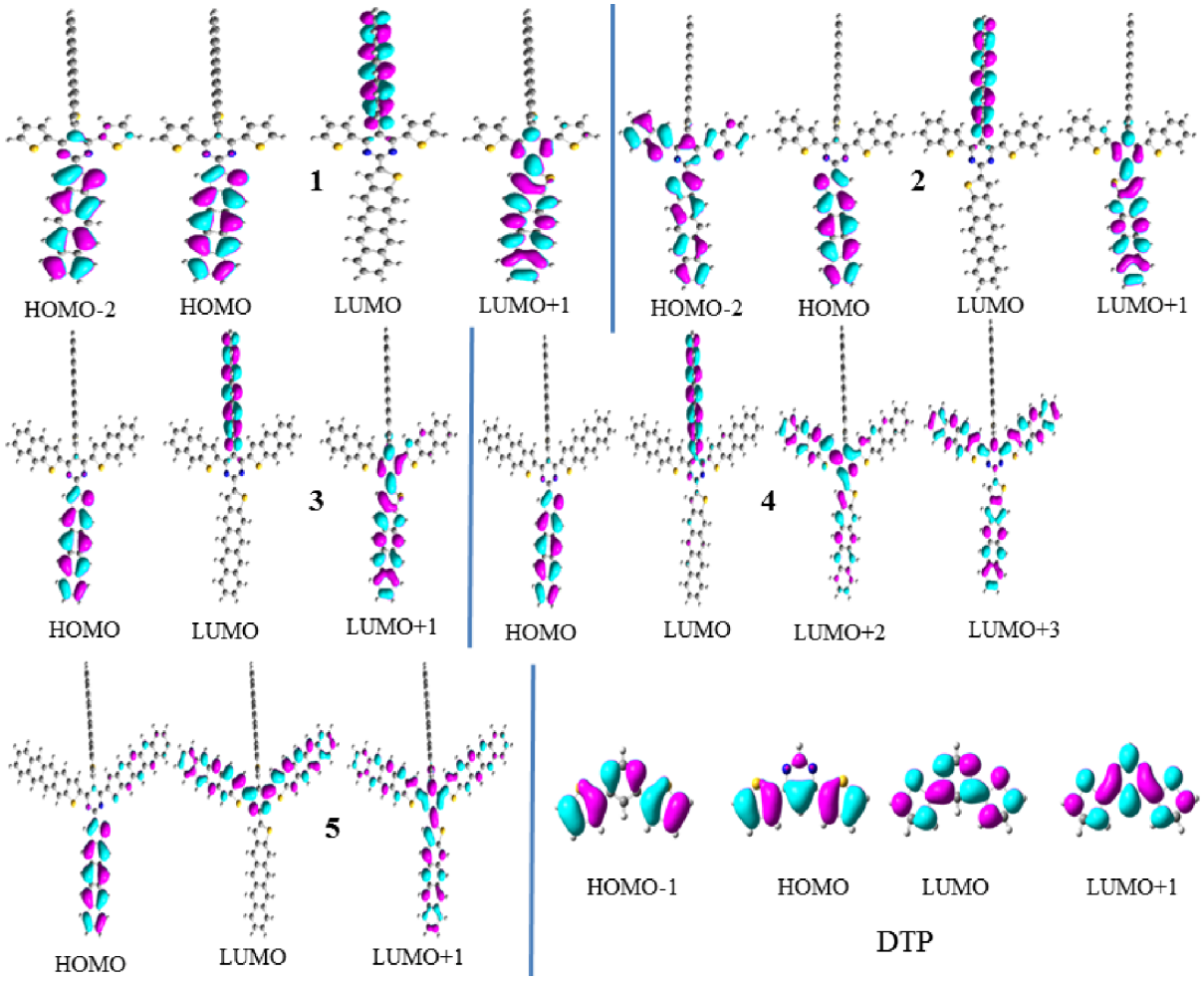

Fig. 2. Distribution pattern of the frontier molecular orbitals of the parent compound DTP and its derivatives **1**-**5** at the ground state

The charge density distribution of FMOs for DTP and its derivatives at the S_0 and S_1 are illustrated in Fig. 2. At S_0, the HOMO is mainly delocalized at thiophene moiety while LUMO is localized at whole DTP compound revealing comprehensible ICT from thiophene to pyrimidine ring. In **1**, ICT was observed from tetracenothiophene (*HOMO*-2) to pyrimidine ring (*LUMO*+1) for the major transitions involved in absorption spectra. In **2**, ICT was observed from benzothiophene (*HOMO*-2) to pyrimidine ring (*LUMO*+1) for the major transitions involved in absorption spectra. In **3**, ICT was observed from tetracenothiophene (*HOMO*) to pyrimidine ring (*LUMO*+1) for the major transitions involved in absorption spectra. In **4**, ICT was observed from tetracenothiophene (*HOMO*) to anthracenothiophene side rings as well as pyrimidine ring (*LUMO*+3) for the major transitions involved in absorption spectra. In **5**, ICT was observed from tetracenothiophene (*HOMO*) to tetracenothiophene of side rings as well as pyrimidine ring (*LUMO*+1) for the major transitions involved in absorption spectra

3.2. Photophysical properties

The computed absorption wavelengths (λ_a) and fluorescence wavelengths (λ_f), oscillator strengths (f) and transitions have been tabulated in Table 2. The calculated λ_a and λ_f for parent molecule DTP are 327 and 353 nm [18] which are in good agreement with the experimental data, i.e., 329 and 378 nm, respectively [37]. The red shift of 94, 107, 308, 234 and 330 nm was noticed for **1**-5 in the λ_a, respectively. The major transitions for **1-5** are *H*-2 –> *L*+1, *H*-2 –> *L*+1, *H* –> *L*+1, *H* –> *L*+3 and *H* –> *L*+1, respectively. The calculated λ_f values were observed 48, 50, 234, 262 and 262 nm being red shifted than the parent molecule DTP. The major transitions were observed *H*-4 –> *L* and *H*-1 –> *L*+2 for **1** and **2** while *H*-1 –> *L* for **3-5**, respectively. It can be found from Table 2, that the oligocene incorporation significantly tune the optical properties. For all the newly designed compounds broader peaks have been observed revealing multiple orbitals participation in the excitation. On the basis of maximum oscillator strength of fluorescence spectra, it is expected that **1** and **2** might be violet, **3** yellow, **4** and **5** as orange light emitter materials.

TABLE 2

Calculated absorption (λ_a) and fluorescence (λ_f) in (nm) of DTP and its derivatives at the TD-B3LYP/6-31G** level of theory[a]

Complexes	f	λ_a	Transition	f	λ_f	Transition
DTP	0.4158	327	*H* –> *L*	0.4326	353	*H* –> *L*
	0.3545	280	*H*-1 –> *L*+1	0.5006	292	*H*-1 –> *L*
1	0.1413	421	*H*-2 –> *L*+1	0.5977	401	*H*-4 –> *L*
2	0.1486	434	*H*-2 –> *L*+1	0.3107	403	*H*-1 –> *L*+2
				0.1695	584	*H*-1 –> *L*
3	0.1053	635	*H* –> *L*+1	0.1725	587	*H*-1 –> *L*
4	0.1491	561	*H* –> *L*+3	0.2468	615	*H*-1 –> *L*
5	0.1664	657	*H* –> *L*+1	0.2448	615	*H*-1 –> *L*

[a] The experimental absorption wavelength (λ_a) = 329 nm; emission wavelength fluorescence (λ_f) = 378 nm from ref. [34]; f = Oscillator Strength

3.3. Charge transfer properties

The IP and EA are the noteworthy properties which would help to understand the charge transfer barrier. Here, the IP and EA were calculated at B3LYP/6-31G** level of theory and tabulated in Table 3. In organic semiconducting devices higher EA would lead to the higher electron transfer behavior while lower IP is very essential to boost up the hole charge transfer capability. The IPa/IPv and EAa/EAv of studied compounds (**1-5**) were computed and presented in Table 3. The IPa/IPv and EAa/EAv of all the studied compounds are smaller and larger than DTP, respectively resulting lower the charge injection barrier revealing that newly designed derivatives might have better hole and electron charge injection ability than the parent molecule. The reorganization energy is the quantity which is very important for estimation of the ability to carry the charge in solid [32, 38]. The reorganization energy values for electron $\lambda(e)$/hole $\lambda(h)$ calculated at B3LYP/6-31G** level have been given in Table 3. The substantial effect towards lowering the $\lambda(h)$ and $\lambda(e)$ have been perceived in all the studied newly designed derivatives compared to the DTP. The $\lambda(h)$ and $\lambda(e)$ of **1-5** have been compared with well-known referenced compounds to shed some light on the charge transfer behavior of newly designed derivatives. The computed values of $\lambda(h)$ are 0.202, 0.061, 0.033, 0.065, 0.042 and 0.028 eV for DTP, **1**, **2**, **3, 4** and **5**, respectively, whereas the $\lambda(e)$ were evaluated as 0.228, 0.152, 0.091, 0.183, 0.181 and 0.087, respectively. The smaller calculated values of $\lambda(h)$ compared to the $\lambda(e)$ are revealing that all the newly designed derivatives might be good as hole transfer materials. The $\lambda(h)$ of **1** is 47, 45, 39, 35, 33, 57, 85; **2** is 75, 73, 67, 63, 61, 85, 113; **3** is 51, 49, 43, 39, 37, 61, 89; **4** is 66, 64, 58, 54, 52, 76, 104; **5** is 80, 78, 72, 68, 90, 118 meV smaller than the $\lambda(h)$ of benzo[1,2-b:5,4-b^0]dithiophene, naphtho[2,3-b:6,7-b^0]dithiophene, naphtho[2,3-b:7,6-b^0]dithiophene, anthra[2,3-b:7,8-b^0] dithiophene, anthra[2,3-b:8,7-b^0] dithiophene, thieno[2,3-f:5,4-f^0]bis[1]benzothiophene and thieno[3,2-f:4,5-f^0]bis[1]benzothiophene, respectively [18]. The pentacene is efficient hole transfer material. Gruhn et al. showed that reorganization energy is the crucial component that allows pentacene to vindicate the particularly higher hole mobility [39]. The $\lambda(h)$ of pentacene was calculated 0.098 eV [40]. From Table 3, it can be seen that the $\lambda(h)$ of newly designed derivatives **1-5** are 37, 65, 33, 56 and 70 meV smaller than the

TABLE 3

The vertical and adiabatic ionization potentials (IP_v/IP_a), vertical and adiabatic electronic affinities (EA_v/EA_a), hole reorganization energies $\lambda(h)$, and electron reorganization energies $\lambda(e)$ of DTP and its derivatives (in eV) at the B3LYP/6-31G** level of theory

Complexes	IP_a	EA_a	IP_v	EA_v	$\lambda(h)$	$\lambda(e)$
DTP	7.58	0.54	7.68	0.43	0.202	0.228
1	5.56	1.65	5.59	1.57	0.061	0.152
2	5.57	1.72	5.60	1.63	0.033	0.091
3	5.56	1.78	5.60	1.68	0.065	0.183
4	5.52	1.83	5.54	1.73	0.042	0.181
5	5.38	1.91	5.39	1.87	0.028	0.087

pentacene, respectively revealing that all the new designed DTP derivatives might be good/comparable hole transfer materials to pentacene. Additionally, the computed $\lambda(e)$ of well-known and commonly used electron transfer material meridional-tris(8-hydroxyquinoline)aluminum (*mer*-Alq3) is 0.276 eV [41]. We found that the $\lambda(e)$ values of **1**-**5** are 124, 185, 93, 95 and 189 meV smaller than the *mer*-Alq3) indicating that electron mobility of these derivatives might be better/comparable with *mer*-Alq3.

3.4. Density of states

For comprehensive understanding of the electronic structures, we have calculated explicit contributions for the individual parts in the form of their TDOS and PDOS shown in (see Fig. 3). We describe two fragments for the parent DTP molecule; fragment one is the central pyrimidine ring, while fragment two contains two thiophene rings. On the other hand three fragments

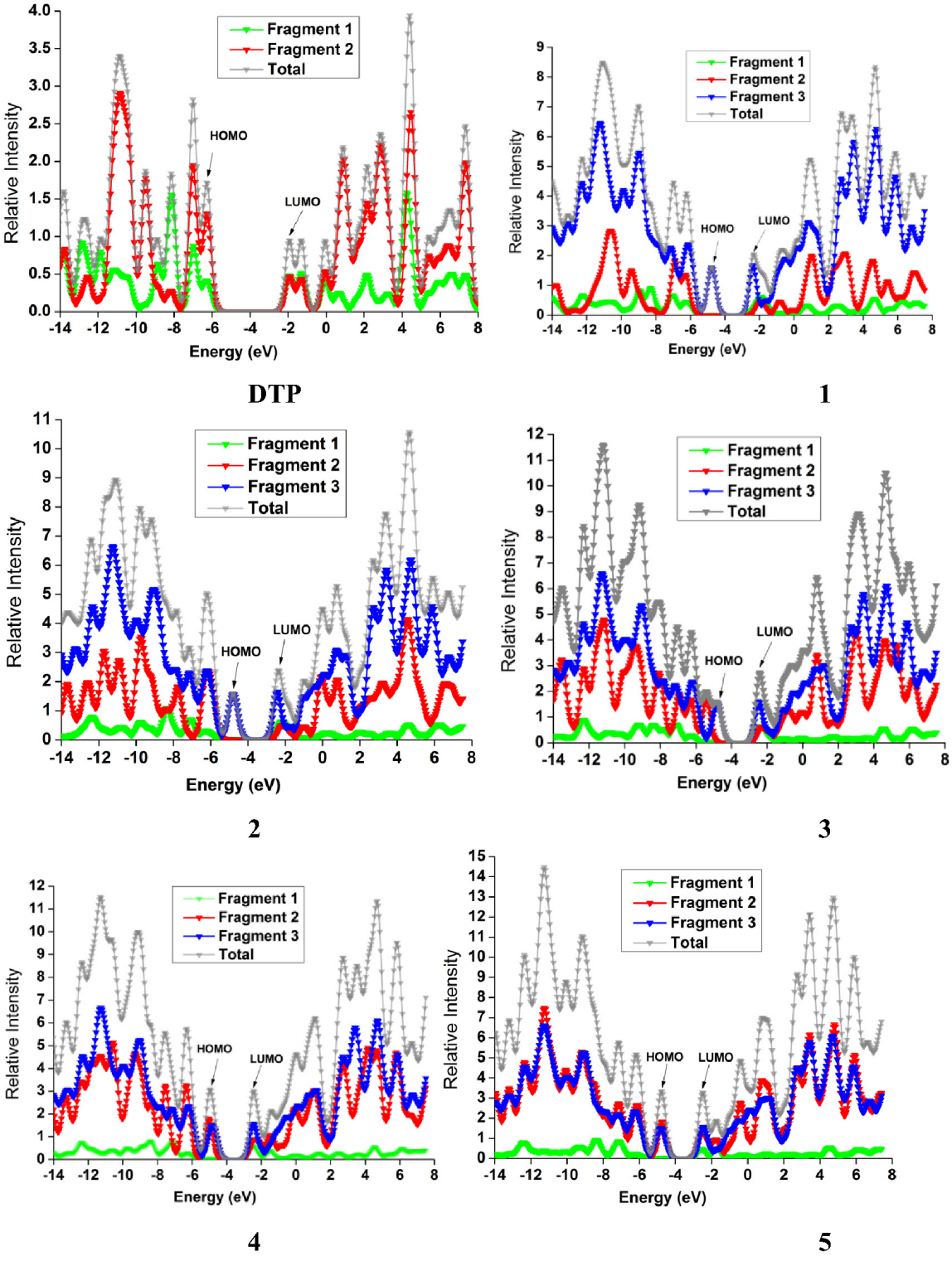

Fig. 3. Graphical representation of TDOS and PDOS for all derivatives

have been defined for molecules **1-5**; fragment one is the central pyrimidine ring; fragment two contains benzothiophene, naphthothiophene, anthracenothiophene and tetracenothiophene for **1-5**, respectively, whereas fragment three consists of the two tetracenothiophene wings (see Fig. 3). The individual fragment represents its contribution to the TDOS of the whole molecule with different curves, see Fig. 3.

As shown in Fig. 3, for DTP, the major contribution from the fragment one (central pyrimidine ring) is between –9 to –8 eV in valance bands and at –4 eV in conduction bands, similarly the peaks from –12 to –6 eV in valance band and from 0 to 8 eV in conduction bands are due to the fragment two. In derivative 1-5 the fragment 1 and the fragment 3 are same so they have the similar kind of contribution in TDOS and PDOS for all derivatives as shown in Fig. 3.

In derivative **1**, the fragment two is contributing in lower valance bands from –12 to –7 eV; while in conduction bands, the peaks from 1 to 7 eV are also from thiophene rings of fragment two. In derivative **2**, the peaks between –14 to –6 eV in the valance bands and the peaks from 0 to 7 eV in the conduction bands are contribution from the fragment two (benzothiophen rings). Similar kind of contribution has been observed for derivatives **3**, **4** and **5** in valance as well as conduction bands with increased intensity due to the enlargement of fragments two, which are naphthothiophene, anthracenothiophene and tetracenothiophene for derivatives **3**, **4** and **5**, respectively.

3.5. Molecular electrostatic potential

The Molecular electrostatic potential (MEP) is a convenient property to investigate the reactivity of derivatives and mapped for all derivatives as shown in Fig. 4. The pink color indicates the higher negative regions that are advantageous for electrophilic attack, while the green color specifies the maximum positive potential regions and these are promising for nucleophilic attack, respectively. The MEP decreases in the order blue > green > yellow > orange > red, while the red color indicates the strongest repulsion and the blue illustrates the ample attraction. This MEP is actually a physical visible property, which could be experimentally accomplished through diffraction approaches [42,43] also by the computational methods. MEP exemplifies the comprehensive distribution for electronic and nuclear charge for a material and is very suitable feature for investigating the reactivity of a certain derivative [44]. In all the derivatives we witnessed that the maximum negative electrostatic potential is

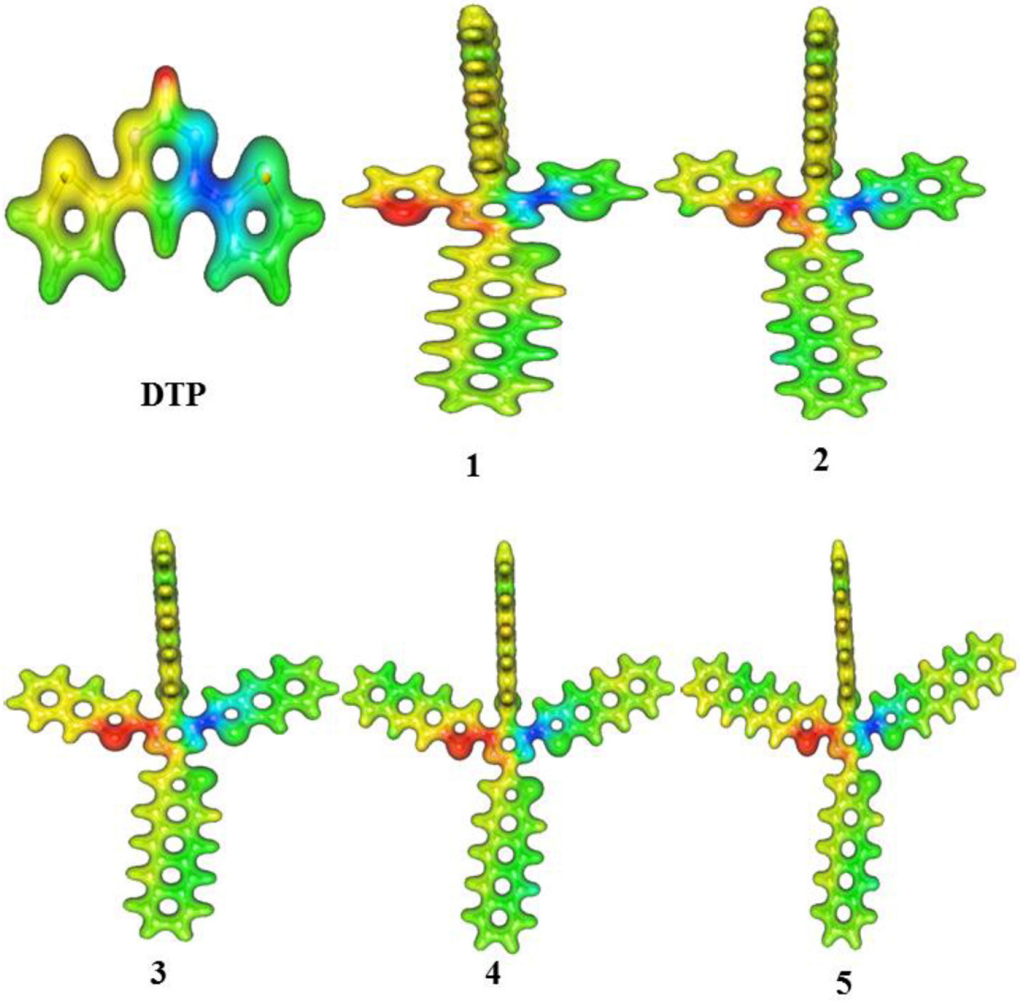

Fig. 4. Molecular electrostatic potential surfaces of all molecules

scattered on the sulpher atoms only, that may be because of the present lone pair at sulpher atoms (see Fig. 4). These results reveal that the significant repulsion is at sulpher atoms whereas the significant attraction is near nitrogen atoms.

4. Conclusions

The optoelectronic and charge transfer properties of DTP were successfully tuned by introduction/incorporation and elongation oligocene/oligocenothiophene core(s). The fusion of benzene, naphthalene, anthracene and tetracene at side wings of compound **1** also decrease the energy gap resulting tuning the photophysical properties. The electron and hole injection ability was successfully enhanced by lowering the LUMO energy level and incorporation the oligocene units. Comprehensible ICT was observed from occupied to unoccupied molecular orbitals. The experimental absorption and fluorescence spectra of parent compound was successfully reproduced by TD-B3LYP/6-31G** level of theory. It is anticipated that compounds **1** and **2** might be violet, **3** yellow, **4** and **5** orange light emitters. The HOMO energies, LUMO energies, IP and EA values showed that newly designed derivatives would have superior hole and electron charge injection ability than the parent compound. The smaller $\lambda(h)$ values than $\lambda(e)$ revealed that newly designed compounds would be good hole transfer contenders. The $\lambda(h)$ of newly designed derivatives are smaller than the pentacene illuminating that prior compounds might be good/comparable hole transfer materials to that of pentacene. The $\lambda(e)$ values of **1-5** are also smaller than the *mer*-Alq3 (an electron transfer materials) indicating that electron mobility of earlier compounds might be better/comparable with *mer*-Alq3. This quantum chemical study would also help to design efficient optoelectronic and charge transfer semiconducting materials.

Acknowledgements

The authors extend their appreciation to the Deanship of Scientific Research at King Khalid University for funding this work through research groups program under grant number R.G.P.1/18/38. A. R. C. is grateful to University of Bisha (UB) for providing the support and facilities to complete the research study.

REFERENCES

[1] W. Li, Z. Wang, P. Lu, Opt. Mater. **26**, 243 (2004).

[2] S. Guang, S. Yin, H. Xu, W. Zhu, Y. Gao, Y. Song, Dyes Pigm. **73**, 285 (2007).

[3] M. Erouel, K. Diallo, J. Tardy, P. Blanchard, J. Roncali, P. Frère, N. Jaffrezic, Materials Science and Engineering: C **28**, 965 (2008).

[4] Y. Xiong, M. Wang, X. Qiao, J. Li, H. Li, Tetrahedron **71**, 852 (2015).

[5] A. Tigreros, A. Ortiz, B. Insuasty, Dyes Pigm. **111**, 45 (2014).

[6] P. Szlachcic, K.S. Danel, M. Gryl, K. Stadnicka, Z. Usatenko, N. Nosidlak, G. Lewińska, J. Sanetra, W. Kuźnik, Dyes Pigm. **114**, 184 (2015).

[7] S.-Y. Gwon, B.A. Rao, H.-S. Kim, Y.-A. Son, S.-H. Kim, Spectrochimica Acta A **144**, 226 (2015).

[8] X.-Q. Ran, J.-K. Feng, A.-M. Ren, W.-C. Li, L.-Y. Zou, C.-C. Sun, J. Phys. Chem. A **113**, 7933 (2009).

[9] A. Irfan, A.G. Al-Sehemi, S. Muhammad, Synth. Met. **190**, 27 (2014).

[10] A. Irfan, A.G. Al-Sehemi, M.S. Al-Assiri, J. Fluorine Chem. **157**, 52 (2014).

[11] J. Zhang, G. Wu, C. He, D. Deng, Y. Li, J. Mater. Chem. **21**, 3768 (2011).

[12] H. Minemawari, T. Yamada, H. Matsui, J.y. Tsutsumi, S. Haas, R. Chiba, R. Kumai, T. Hasegawa, Nature **475**, 364 (2011).

[13] D.H. Kim, Y.D. Park, Y. Jang, H. Yang, Y.H. Kim, J.I. Han, D.G. Moon, S. Park, T. Chang, C. Chang, M. Joo, C.Y. Ryu, K. Cho, Adv. Funct. Mater. **15**, 77 (2005).

[14] L. Wang, G. Nan, X. Yang, Q. Peng, Q. Li, Z. Shuai, Chem. Soc. Rev. **39**, 423 (2010).

[15] J.E. Anthony, Angew. Chem. Int. Ed. **47**, 452 (2008).

[16] J.E. Anthony, Chem. Rev. **106**, 5028 (2006).

[17] J. Mei, Y. Diao, A.L. Appleton, L. Fang, Z. Bao, J. Am. Chem. Soc. **135**, 6724 (2013).

[18] A. Irfan, A. Rasool Chaudhry, A. G. Al-Sehemi, M. Sultan Al--Asiri, S. Muhammad, A. Kalam, J. Saudi. Chem. Soc. **20**, 336 (2016).

[19] A. Irfan, A. Kalam, A.R. Chaudhry, A.G. Al-Sehemi, S. Muhammad, Optik – Intern. J. Light Elect. Optics **132**, 101 (2017).

[20] A. Irfan, A.G. Al-Sehemi, A.R. Chaudhry, S. Muhammad, Optik – Intern. J. Light Elect. Optics **138**, 349 (2017).

[21] W. Kohn, A.D. Becke, R.G. Parr, J. Phys. Chem. **100**, 12974 (1996).

[22] A.D. Becke, J. Chem. Phys. **98**, 5648 (1993).

[23] R.S. Sánchez-Carrera, V. Coropceanu, D.A. da Silva Filho, R. Friedlein, W. Osikowicz, R. Murdey, C. Suess, W.R. Salaneck, J.-L. Brédas, J. Phys. Chem. B **110**, 18904 (2006).

[24] C. Lee, W. Yang, R.G. Parr, Phys. Rev. B **37**, 785 (1988).

[25] G.A. Petersson, A. Bennett, T.G. Tensfeldt, M.A. Al-Laham, W.A. Shirley, J. Mantzaris, J. Chem. Phys. **89**, 2193 (1988).

[26] F. Furche, R. Ahlrichs, J. Chem. Phys. **117**, 7433 (2002).

[27] A. Irfan, A.G. Al-Sehemi, S. Muhammad, A.R. Chaudhry, M.S. Al--Assiri, R. Jin, A. Kalam, M. Shkir, A.M. Asiri, Comptes Rendus Chimie (2015).

[28] C. Zhang, W. Liang, H. Chen, Y. Chen, Z. Wei, Y. Wu, J. Mol. Struct. (TheoChem) **862**, 98 (2008).

[29] A.R. Chaudhry, R. Ahmed, A. Irfan, A. Shaari, A.G. Al-Sehemi, Mater. Chem. Phys. **138**, 468 (2013).

[30] R.A. Marcus, N. Sutin, Biochim. Biophys. Acta – Rev. Bioenerg. **811**, 265 (1985).

[31] E.V. Tsiper, Z.G. Soos, W. Gao, A. Kahn, Chem. Phys. Lett. **360**, 47 (2002).

[32] J.L. Brédas, J.P. Calbert, D.A. da Silva Filho, J. Cornil, Proc. Natl. Acad. Sci. **99**, 5804 (2002).

[33] R. Jin, A. Irfan, RSC Advances **7**, 39899 (2017).
[34] A. Irfan, A.R. Chaudhry, S. Muhammad, A.G. Al-Sehemi, J. Mol. Graphics Modell. **75**, 209 (2017).
[35] S.H. Frisch MJ, et al.,, , in, Gaussian 09, Revision A. 01,, Gaussian Inc., Wallingford, CT, 2009.
[36] S. Muhammad, A.R. Chaudhry, A. Irfan, A.G. Al-Sehemi, RSC Advances **7**, 36632 (2017).
[37] G.S.H. S. Dufresne, W.G. Skene, J. Phys. Chem. B **111**, 11407 (2007).
[38] R.A. Marcus, Rev. Mod. Phys. **65**, 599 (1993).
[39] N.E. Gruhn, D.A. da Silva Filho, T.G. Bill, M. Malagoli, V. Coropceanu, A. Kahn, J.-L. Brédas, J. Am. Chem. Soc. **124**, 7918 (2002).
[40] S.T. Bromley, M. Mas-Torrent, P. Hadley, C. Rovira, J. Am. Chem. Soc. **126**, 6544 (2004).
[41] A. Irfan, R. Cui, J. Zhang, L. Hao, Chem. Phys. **364**, 39 (2009).
[42] P. Politzer, D.G. Truhlar (Eds.), Plenum Press, New York (1981).
[43] R.F. Stewart, Chem. Phys. Lett. **65**, 335 (1979).
[44] J.S. Murray, P. Politzer, WIRES Comput. Mol. Sci. **1**, 153 (2011).